

UKAEA-CCFE-CP(23)64

V.G. Kiptily, P.J. Bonfigliolo, T. Craciunescu, J.
Eriksson, M. Fitzgerald, V. Goloborodko, M.
Nocente, S. Menmuir, M. Podestà, M. Poradzinski, D.
Rigamonti, Z. Stancar, S.E. Sharapov, H. Sun, D.M.
Taylor, M. Tardocchi, P. Beaumont, et al.

OBSERVATION OF ALPHA PARTICLES IN DT- AND T-PLASMAS ON JET

This document is intended for publication in the open literature. It is made available on the understanding that it may not be further circulated and extracts or references may not be published prior to publication of the original when applicable, or without the consent of the UKAEA Publications Officer, Culham Science Centre, Building K1/O/83, Abingdon, Oxfordshire, OX14 3DB, UK.

Enquiries about copyright and reproduction should in the first instance be addressed to the UKAEA Publications Officer, Culham Science Centre, Building K1/O/83 Abingdon, Oxfordshire, OX14 3DB, UK. The United Kingdom Atomic Energy Authority is the copyright holder.

The contents of this document and all other UKAEA Preprints, Reports and Conference Papers are available to view online free at scientific-publications.ukaea.uk/

OBSERVATION OF ALPHA PARTICLES IN DT- AND T-PLASMAS ON JET

V.G. Kiptily, P.J. Bonfiglio, T. Craciunescu, J. Eriksson, M.
Fitzgerald, V. Goloborodko, M. Nocente, S. Menmuir, M. Podestà,
M. Poradzinski, D. Rigamonti, Z. Stancar, S.E. Sharapov, H. Sun,
D.M. Taylor, M. Tardocchi, P. Beaumont, et al.

OBSERVATION OF ALPHA PARTICLES IN D-T AND T-PLASMAS ON JET

V.G. KIPTILY¹, C.D. CHALLIS¹, R. DUMONT², M. FITZGERALD¹, J. GARCIA², L. GARZOTTI¹, Z. GHANI¹, J. HOBIRK³, P. JACQUET¹, A. KAPPATOU³, D. KEELING¹, YE. KAZAKOV⁴, P. MANTICA⁵, M.J. MANTSINEN^{6,7}, S.E. SHARAPOV¹, E.R. SOLANO⁸, D. VAN EESTER⁴, P.J. BONOFIGLO⁹, T. CRACIUNESCU¹⁰, A. DAL MOLIN¹¹, J. ERIKSSON¹², V. GOLOBORODKO¹³, M.V. ILIASOVA¹⁴, E.M. KHILKEVITCH¹⁴, M. NOCENTE¹¹, S. MENMUIR¹, M. PODESTÀ⁹, M. PORADZINSKI¹, D. RIGAMONTI¹⁵, J. RIVERO-RODRIGUEZ^{1,16}, Z. STANCAR^{1,17}, A.E. SHEVELEV¹⁴, P. SIREN¹, H. SUN¹, D.M. TAYLOR¹, M. TARDOCCI¹⁵, P. BEAUMONT¹, F. BELLI¹⁸, F.E. CECIL¹⁹, R. COELHO²⁰, M. CURUIA²¹, M. GARCIA-MUNOZ¹⁶, E. JOFFRIN², D. KING¹, C. LOWRY¹, M. LENNHOLM¹, E. LERCHE⁴, C.F. MAGGI¹, J. MAILLOUX¹, D. MAROCCO¹⁸, M. MASLOV¹, C. PEREZ VON THUN²², F. RIMINI¹ and JET CONTRIBUTORS*

¹ UKAEA, Culham Science Centre, Abingdon, Oxfordshire, OX14 3DB, UK

² CEA, IRFM, F-13108 Saint-Paul-Lez-Durance, France

³ Max-Planck-Institut für Plasmaphysik, Boltzmannstr. 2, 85748 Garching, Germany

⁴ LPP-ERM/KMS, Association EUROFUSION-Belgian State, TEC partner, Brussels, Belgium

⁵ Istituto per la Scienza e Tecnologia Dei Plasmi, Consiglio Nazionale Delle Ricerche, Milano, Italy

⁶ Barcelona Supercomputing Centre, Barcelona, Spain

⁷ ICREA, Pg. Lluís Companys 23, 08010 Barcelona, Spain

⁸ Laboratorio Nacional de Fusión, CIEMAT, Madrid, Spain

⁹ Princeton Plasma Physics Laboratory, Princeton, NJ 08543, New Jersey, USA

¹⁰ National Institute for Laser, Plasma and Radiation Physics, Bucharest, Romania

¹¹ Dipartimento di Fisica, Università di Milano-Bicocca, Milan, Italy

¹² Department of Physics and Astronomy, Uppsala University, BOX 516, Uppsala, Sweden

¹³ Kyiv Institute for Nuclear Research, Prospekt Nauky 47, Kyiv 03680, Ukraine

¹⁴ Ioffe Physico-Technical Institute, 26 Politekhnicheskaya, St Petersburg 194021, Russia

¹⁵ Institute for Plasma Science and Technology, National Research Council, Milan, Italy

¹⁶ FAMN Department, Faculty of Physics, University of Seville, 41012 Seville, Spain

¹⁷ Jožef Stefan Institute, Jamova 39, SI-1000 Ljubljana, Slovenia

¹⁸ Unità Tecnica Fusione -ENEA C. R. Frascati -via E. Fermi 45, 00044 Frascati (Roma), Italy

¹⁹ Colorado School of Mines, Golden, CO 80401, USA

²⁰ Instituto de Plasmas e Fusão Nuclear, Instituto Superior Técnico, Universidade de Lisboa, 1049-001 Lisboa, Portugal

²¹ National Institute for Cryogenics and Isotopic Technology, Bucharest, Romania

²² Forschungszentrum Jülich GmbH, Institut für Energie- und Klimaforschung-Plasmaphysik, 52425 Jülich, Germany

*See the author list of “Overview of T and D-T results in JET with ITER-like wall” by CF Maggi et al. to be published in Nuclear Fusion Special Issue: Overview and Summary Papers from the 29th Fusion Energy Conference (London, UK, 16-21 October 2023)

Email: Vasili.Kiptily@ukaea.uk

Abstract

The fusion reaction between deuterium and tritium, $D(T,n)^4He$ is the main source of energy in future thermonuclear reactors. 4He -ions (α -particles) born with an average energy of 3.5 MeV, transferring energy to the thermal plasma during their slowing down, should provide the self-sustained D - T plasma burn. That is why the α -particle studies have been a priority task for the second D - T experiments (DTE2) on Joint European Tokamak (JET) to understand the main mechanisms of their slowing down, redistribution and losses and to develop optimal plasma scenarios for reactors. Enhanced α -particle diagnostics on JET allowed to obtain several novel results that will be presented in the paper.

1. INTRODUCTION

The fusion reaction between deuterium (D) and tritium (T), $D(T,n)^4He$ is the main source of energy (≈ 17.6 MeV per fusion) in future thermonuclear reactors. The charged fusion product of this reaction, 4He -ions (α -particles), born with energy of ≈ 3.5 MeV, should provide the self-sustained D - T plasma burn, transferring energy to the thermal plasma during their slowing down. An adequate confinement of α -particles is essential to provide efficient heating of the bulk plasma and steady burning of a reactor plasma. That is why the fusion-born α -particle studies on JET were a priority task for DTE2 the second D - T experiments on Joint European Tokamak (JET). The goal is to understand the main mechanisms of their slowing down, redistribution and losses developing optimal, energy effective plasma scenarios for International Thermonuclear Experimental Reactor (ITER) and future fusion

reactors with magnetic confinement. JET, with the ITER-like wall (beryllium wall with tungsten divertor) and enhanced auxiliary heating systems, produced significant population of α -particles in plasmas and provided a great opportunity to study the α -particle behaviour, giving a step-ladder approach for modelling and extrapolating to ITER.

The full-scale D - T experiments on the tokamak fusion test reactor (TFTR) [1] and JET [2] in 1997 (DTE1) has shown that direct measurements of alphas are very difficult. Alpha-particle studies require a significant development of dedicated diagnostics for both confined and lost α -particles. To make such measurements possible JET, being a testbed for ITER, was equipped with a dedicated set of fast α -particle diagnostics for operation at the high neutron and γ -ray fluxes in the D - T experiments. The detailed description of the α -particle diagnostics can be found in the next section.

Selected new results of α -particle studies in DTE2 are presented in this paper. Direct evidence of the α -particle self-heating [3] is given in the Section 3. Confinement of fast α -particles produced in fusion reactions is of crucial importance for reactors. Plasma instabilities may lead to significant α -particle losses and the loss of plasma heating that is not acceptable for the efficient fusion plant as it can cause problems with ignition and damage to the first wall. In Section 4 we present the α -particle loss effects related to MHD activity in D - T plasmas. Fusion γ -rays, 17-MeV γ -rays due to the $D(T,\gamma)^4\text{He}$ reaction and 20-MeV γ -rays of the $T(H,\gamma)^4\text{He}$ reaction, were measured in D - T and tritium plasmas with the H -minority heating. These important results obtained for the first time are shown in the Section 5. Finally, a summary and conclusions of the paper are presented in the last Section.

2. ALPHA-PARTICLE DIAGNOSTICS

The first full scale D - T experiment on JET in 1997 (DTE1) has shown that direct measurements of confined and lost alphas are very difficult and α -particle studies require a substantial development of dedicated diagnostics. To make such measurements available in DTE2, JET was equipped with a set of fast α -particle diagnostics for operation at the high neutron and γ -ray fluxes in D - T experiments.

2.1. Alpha-particle source profile measurements

The JET plasma heating, with beam injection of the energetic deuterium and tritium neutrals (NBI) and with waves in the ion-cyclotron range of frequencies (ICRF), assumes that in some plasma scenarios the beam-target fusion reaction rate could be substantial, so the energetic ion power deposition and, hence, the α -particle source profile measurements are rather important for dedicated studies of the confined and lost α -particles. An exciting evolution of the D - T α -particle source has been measured with JET 2D neutron camera during D -NBI heating of the D -plasma with T -puff [4]. Also, plasma instabilities, for example, sawtooth oscillations, interacting with D -beam ions accelerated by ICRF are causing a dramatic D - ^3He α -particle source profile change [5].

The JET neutron profile monitor [6, 7] consists of 2 fan-shaped array cameras with 19 collimated viewing channels (9 vertical and 10 horizontal), which has 2 independent rotatable collimators with 10- and 21-mm apertures each. Viewing width in the poloidal plane, depending on the collimator apertures, is ~ 5 –10 cm in the central channels and is ~ 10 –20 cm in the edge channels. The plasma coverage is acceptable for tomography reconstructions. Two sets of neutron detectors, NE213 liquid scintillators used for 2.5-MeV D - D and 14-MeV D - T neutrons and BC418 plastic scintillators for D - T neutrons detection, are available. Both sets equipped with individual digital data acquisition systems that allow measurements in DTE2. Also, in front of the neutron detectors can be setup γ -ray spectrometers, which are placed on a movable rail.

2.2. Fusion gamma-ray spectrometers

Gamma-ray diagnosis is one of the important techniques used on JET for studying confined fast ions [8]. Four high-performance γ -ray spectrometers were installed on JET. Three of them, $\text{LaBr}_3(\text{Ce})$ scintillators and HpGe -detector (a high purity Ge -detector is placed on a remotely controlled slider sharing the same line-of-sight with the scintillator) are viewing the plasma centre vertically through 2-m collimators equipped with neutron attenuators. The fourth one, $\text{LaBr}_3(\text{Ce})$ scintillator with tangential field of view with an improved neutron attenuation [9]. The $\text{LaBr}_3(\text{Ce})$ scintillator has a short decay time of ~ 20 ns, a high photo-yield. The $\text{LaBr}_3(\text{Ce})$ spectrometers have the counting rate limit ~ 1 MHz, and at the same time a high energy resolution [10]. The γ -ray spectra are continuously recorded in all JET discharges over the energy range 1-30 MeV.

2.3. Fast ion loss detectors (FILDs)

Two devices have been installed in the JET vacuum vessel near the plasma boundary to measure the loss of energetic ions and fusion products, in particular α -particles during the D - T experiments. First detector is an array of multichannel thin-foil charge collectors (Faraday Cups) with poloidal, radial and energy resolution [11, 12]. Second one is a well collimated scintillator probe (SP) providing gyro-radius (G-R) (energy) and pitch-angle (P-A) resolution, which is optically connected to a charge-coupled device (CCD) and array of 16 photomultipliers (PMT) equipped with 2-MHz digitisers [13, 14]. The high-frequency digitisers have allowed comparing both fusion-product losses and Mirnov coil spectrograms to identify the resonant MHD modes [15]. These diagnostics provided novel α -particle observations in DTE2.

3. ALPHA-PARTICLE HEATING

In high-power TFTR experiments [16, 17] were found that the energy stored in the electron and ions increased by $\sim 20\%$ in the $n_D \approx n_T$ plasma compared to similar pure deuterium plasmas. It was stated that the increase took place both due to improved confinement associated with the use of tritium, and probably heating of electrons by D - T α -particles. Later, in DTE1 experiments with the fuel mixture scan, separating the effects of improved confinement and α -particle heating [18], the α -particle heating effects were seen in the electron temperature and energy content.

In the recent DTE2 experiments the direct α -particle self-heating was identified in high-performance plasma discharges with power modulation of D - and T -NBI but without ICRF heating [3]. It was observed that in the NBI afterglow period the total neutron rate (substantially D - T neutrons) is decreasing while the plasma core electron temperature, $T_e(0)$, measured by the electron cyclotron emission (ECE) diagnostics, is still increasing for a short period. This evolution is in a contrast to the reference high-performance deuterium discharges with D -NBI heating, in which both T_e and D - D neutron rate are decreasing during the NBI afterglow.

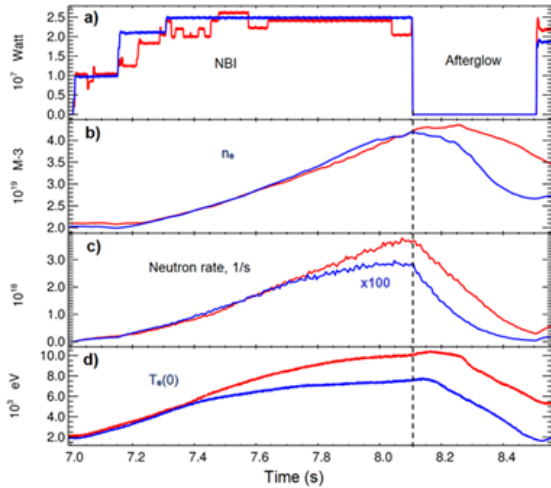


Figure 1. Waveforms of the D - T JET pulse #99801 (red solid lines) vs the deuterium JET pulse #100793 (blue solid lines). Panels show waveforms of the NBI heating power, the central electron temperature, $T_e(0)$ and the measured neutron rate.

As can be seen from figure 1d, at the top performance of the D - T discharge, the core electron temperature gain is about 30% ($\Delta T_e(0) \approx 2.5$ keV) at same heating conditions with deuterium discharge. As it was declared in [16-18], this T_e increase happen both due to improved confinement associated with the use of tritium and heating of electrons by D - T fusion α -particles. In the afterglow period, the D - T core electron temperature has a trend with $dT_e/dt \geq 0$ during the first $t \approx 60$ ms of the D - T afterglow, reaching $T_e(0) \approx 10.3$ keV. In the next ~ 70 ms the core temperature is slightly decreasing to ~ 10 keV and then, it is falling rather rapidly, but not so fast as in the reference deuterium discharge. Thus, during the first ~ 130 ms of the afterglow, the core electron temperature of the D - T plasma remained in the range 10 – 10.3 keV without any neutral beam injection. We should note that slowing down of the 3.5-MeV α -particles is predominantly due to electron friction since their energy $E_\alpha \gg E_{crit} \approx 0.38$ MeV (according to [19], at the critical energy of ions, E_{crit} , the rate of loss of energy to the plasma electrons and to the ions is equal). At the same time, thermalisation of NBI ions occurs mainly due to interaction with fuel ions because of $E_{T-NBI} < E_{crit} \approx 0.31$ MeV and $E_{D-NBI} < E_{crit} \approx 0.21$ MeV. Hence, the D - and T -beam ions are mostly heating the plasma fuel ions, merely 3.5-MeV D - T α -particles could heat electrons in the plasma core that shown in figure 1d. The ion-electron slowing down time of 3.5-MeV

A detailed analysis of the observed effect has been performed for the hybrid D - T discharge #99801 fuelled with approximately equal densities of deuterium and tritium, $n_D \approx n_T$, and the reference deuterium discharge #100793. Waveforms of NBI power, n_{e0} , $T_e(0)$ and neutron rate are presented in figure 1. Both discharges were delivered at the toroidal magnetic field $B_0=3.45$ T on the magnetic axis, plasma current is $I_p=2.3$ MA, the safety factor in the core was $q(0)\sim 1$ and the electron density $n_{e0} \approx 4.3 \times 10^{19} \text{ m}^{-3}$, a central line averaged density measured by far infrared diagnostic system. The neutral D - and T -beams with energies $E_{NBI} \approx 105$ -115 keV were injected to heat the fuel ions. A maximum NBI heating power of $P_{NBI} \approx 26$ MW was injected by radial and tangential neutral beams; the NBI afterglow period was from $t=8.105$ s to $t=8.5$ s (see figure 1a) that is sufficient for beam thermalisation. Note that T -ion slowing down time longer than D -ions by a factor of 3/2 and the difference of neutron-rate decays during the afterglow demonstrate that.

alphas, is $\tau_{s\alpha} \sim 910$ ms. As a result of electron friction during 400 ms, the average α -particle energy loss is ~ 1.8 MeV, so their energy will be $E_\alpha \sim 1.7$ MeV $\gg E_{crit}$. Therefore, D - T α -particles can provide sustainable electron heating during slowing down in the afterglow lasting ≈ 400 ms. The NBI ion thermalisation time is less than 100 ms.

The TRANSP [20] neutron rate calculations show that in the analysed D - T discharge the thermal neutron rate dominates during both the high-performance and the afterglow periods, exceeding the beam-target neutron rate component. Neutron rates in both discharges are decreasing during the afterglow periods. However, in the deuterium afterglow, the neutron rate decays about 2-fold faster than in the D - T afterglow phase.

The TRANSP modelling shows electron heating in both D - T discharge and deuterium discharges (see figure 2).

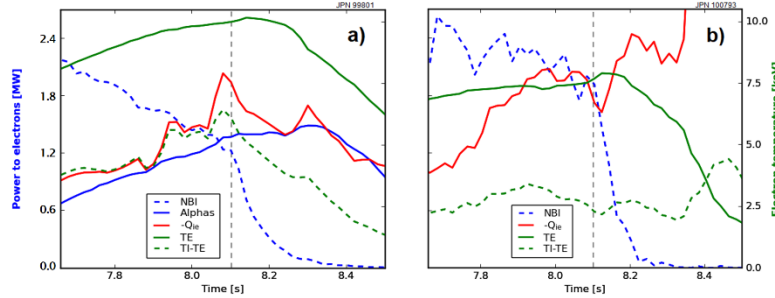


Figure 2. TRANSP analysis of electron heating in JET D - T discharge #99801 (a) and deuterium discharge #100793 (b). The power transferred to electrons (left scale) by alphas, NBI and thermal ions ($-Q_{ie}$) are presented as well as electron temperature on axis (TE) and a difference between the ion and electron temperatures (TI-TE) in the plasma core (right scale).

The power transferred to electrons by alphas, NBI and the equipartition power exchange between ions and electrons, Q_{ie} , were obtained for the plasma core, in the range of the dimensionless radius $\rho \equiv \sqrt{\psi_{tor}^{norm}} < 0.05$ (ψ_{tor}^{norm} is a normalized toroidal magnetic flux). The D - T discharge modelling shows that the α -particle power transfer grows during the NBI heating phase and keep growing ≈ 200 ms in afterglow up to ≈ 1.5 MW. At the same time, the NBI power transfer to electrons is dropping down. There is not a credible change of ΔT in the deuterium case. Also, TRANSP

shows that in the D - T discharge Q_{ie} , the equipartition power exchange between ions and electrons, in the core is comparable to the α -particle power transfer contribution. We need to note that an assessed Q_{ie} uncertainty is about 30% as far as measured and extrapolated T_i errors are rather high in the plasma core. The transport modelling of the D - T and deuterium discharges is consistent with experimental measurements despite large error bars of the input data. So, the α -particle self-heating effect was confirmed in the high-performance D - T discharges with NBI power afterglow.

4. ALPHA-PARTICLE LOSSES

4.1. Fishbone α -particle losses

During development of a high-performance hybrid D -plasma scenario for DTE2, an increased level of D - D fusion product non-resonant losses, tritons and protons, in the MeV-energy range was observed during the instability of $n=1$ fishbones [15]. In DTE2, it was also found that α -particle losses are coherent with fishbones. A strong fishbone activity was observed in both the hybrid [21] and the baseline H-mode scenario [22] discharges. An example of the FILD footprint of alphas due to the fishbone is demonstrated in figure 3b. The Fourier analysis shows that α -particle losses are coherent with fishbones (see in figure 3a). It was found that these fishbone losses are related to alphas with energies more than 2 MeV.

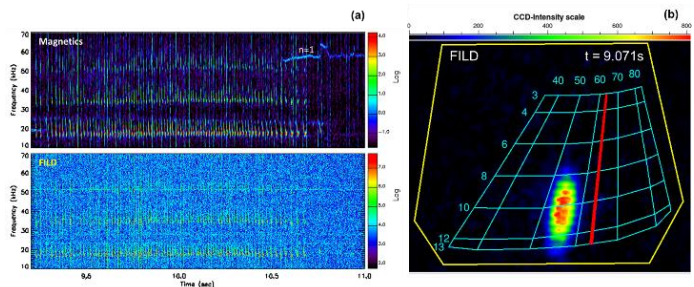


Figure 3. (a) – Fourier spectrograms of in-vessel magnetic pickup-coil (upper box) and FILD (bottom box) signals in JET discharge #99950; (b) – footprint of α -particle losses detected by FILD CCD in JET discharge #99950 due to fishbone; red-line indicates the ICRF resonance layer on the grid.

The high-performance hybrid pulse #99950, set a fusion energy record of ≈ 45.8 MJ with $n_D \approx n_T$ plasma even though a strong $n=1$ fishbone activity continued ≈ 2 s from $t=9$ s. Prompt α -particle losses are dominant, however there are low-energy ions that are also lost due to the $n=1$ fishbones. Note, a continuous decrease of the core temperature, $T_e(0)$, is triggered just after strong fishbones and related sawteeth. Meanwhile, despite the presence of the fishbones the neutron rate grows up until an $n=4$ tearing mode is triggered by a strong ELM.

The similar effect during the fishbone activity have been observed in the JET baseline H-mode scenario discharges. For example, in #99948 (3.3T/3.5MA) regardless of a long fishbone activity, the neutron rate is continuously growing up to appearance of a strong $n=4$ continuous mode. So, an additional study of these discharges is required to understand this important fishbone effect.

4.2. ELMs and α -particle losses

Alpha-particle losses, which are correlated with appearance of ELMs, were detected in the high-performance $D-T$ discharges. For example, strong spikes of the *Bell* emission indicating ELM activity were observed in discharge #99449 (3.4T/2.3MA). Basically, the total α -particle loss rate in this discharge follows the neutron rate that indicates the classical first-orbit losses. Nevertheless, there are some loss spikes that coincides with ELMs. Figure 4 shows a differential FILD CCD footprint, which is related to alpha-particles in the energy range $E_\alpha \approx 2.2 - 3.5$ MeV. The back-in-time orbit calculations demonstrate that these α -particles are passing marginally close to the plasma edge and potentially, fast-ion redistribution or loss could cause the ELM instability. Note that the ECE diagnostics confirms a T_e irregularity localised at $R \approx 3.80$ m.

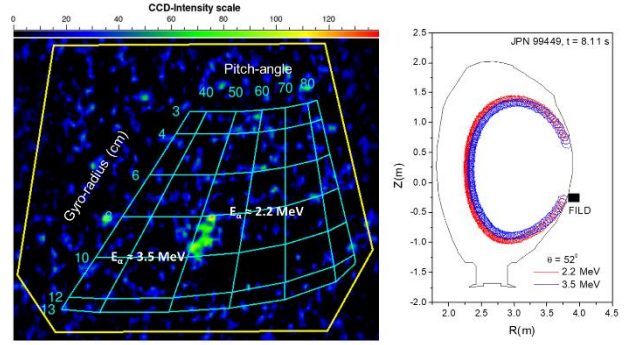


Figure 4. Differential footprint of α -particle losses detected by FILD CCD in JET discharge #99449 at 8.11 s and lost α -particle orbits calculated back-in-time from the footprint.

4.3. Anomalous α -particle losses

In a special “bump-on-tail” experiments [23] ($B_T = 3.7$ T, $I_p = 2.5$ MA) anomalous losses of the MeV-alphas were observed with FILD SP and FC. The main source of α -particles was the beam-target reactions due to modulated injection of 110-keV D - and T -beams ($P_{NBI} \approx 10$ -15 MW) in both T -rich and D -rich L-mode plasmas. Figure 5 shows footprints of α -particle losses recorded with FILD CCD camera in these type discharges. It is clear seen that in both cases the pitch-angle ($\theta = \cos^{-1}(v_{\parallel}/v)$) distribution of losses has “double-hump” features. One can see that a maximal loss rate appears at $\theta \approx 58^\circ$ and $\approx 75^\circ$, whilst the minimal losses are in the range $\theta \approx 62^\circ - 70^\circ$.

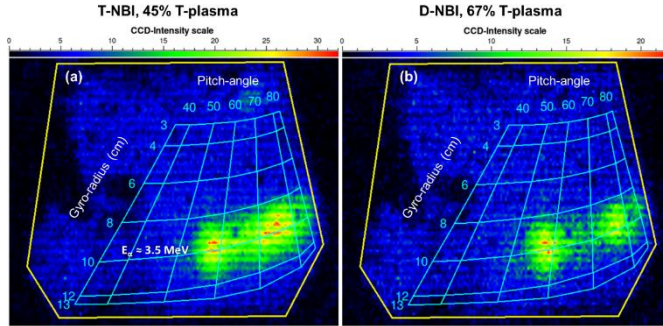


Figure 5. FILD CCD camera images recorded in JET $D-T$ shots with NBI-heating: (a) – #99502, $t = 7.20 - 7.45$ s; (b) – #99503, $t = 8.0 - 8.5$ s.

An important piece of information was obtained with neutron profile measurements that characterise α -particle source. Tomographic reconstructions of the line-integrated $D-T$ neutron emissivities recorded with the 2D neutron camera show that α -particle source profiles have a sort of “shoulders”. The neutron emissivity in these discharges are characterised by a dominated beam-target component. Thus, these profiles may point at anomalous transport of the NBI ions. It

Since the first orbit losses are of the particles with trapped orbits, the major radius at the bounce reflection point for these particles and the pitch-angle value on the scintillator plate are related by $R(\theta) = R_{\text{FILD}}[1 - \cos^2(\theta)]$, where R_{FILD} is radial position of the scintillator plate. So, α -particles related to the plasma regions near to $R(58^\circ) \approx 2.75$ m and $R(75^\circ) \approx 3.6$ m more intensively escape the plasma than α -particles from the $R \approx 3.0 - 3.3$ m, in vicinity of the magnetic axis at $R \approx 3.0$ m. Analysis of interferometry, reflectometry and soft X-ray data indicates high-frequency Alfvénic activity, however no α -particle loss correlations were observed.

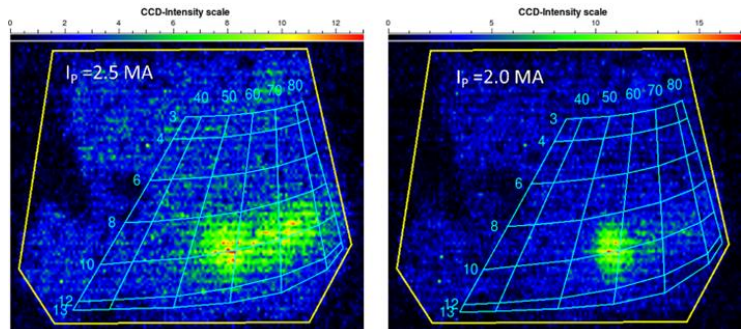


Figure 6. FILD CCD camera images recorded in discharges with 3-ion ICRF heating: (a) – discharge # 99604, $I_p = 2.5$ MA; (b) – discharge #99607, $I_p = 2.0$ MA.

could be a reason why the double-hump α -particle loss pattern is observed.

Surprisingly, the “double-hump” α -particle loss pattern was also observed in the D - T plasma discharges (3.7T/2.5MA) with a novel ICRF heating scheme – 3-ion ICRF heating of Be -impurity that naturally presents in JET ($f_{ICRF}=25$ MHz) [24]. However, there is no double hump in these 3-ion ICRF heating discharges at $I_p = 2.0$ MA (see figure 6). Furthermore, nearly identical neutron profiles confirm both an effective central heating of plasmas with 3-ion ICRF scheme and lack of difference in the fast-ion transport. The physics behind this anomalous α -particle loss pattern is being investigated. Note, the double hump losses have been observed in special ripple experiments on JET [25]. Also, anomalous losses of D - D fusion tritons and protons have been found in some JET plasmas with normal ripples, which normally are very low. Modelling of these discharges demonstrated that fusion products may experience a super-banana diffusion, which is significantly exceeding the neoclassical level [26].

4.4. Spatial and pitch-angle distribution of α -particle losses

An additional information on observation and analysis of coherent and non-coherent α -particle losses due to a variety of low frequency MHD activity as well as a discussion of the loss mechanisms, spatial and pitch dependencies of losses is presented in the conference paper [27].

5. ALPHA-PARTICLES IN TRITIUM PLASMAS

An important part of the fusion-born α -particle studies on JET was tritium plasma experiments. The α -particle spectrum in tritium plasmas is rather complicated because there are several branches of the T - T fusion reaction. Indeed, the $T(T,2n)^4He$ reaction gives rise to neutrons and the MeV α -particles with continuous energy spectra since 3 outgoing particles in the final state providing $\sim 70\%$ of the total T - T reaction rate. The maximal energy of the T - T neutrons is about 9 MeV, whereas α -particles are born in the energy range $E_\alpha \approx 0 - 3.8$ MeV. In addition, there is $\sim 30\%$ contribution of monoenergetic alphas due to the sequence of the $T(T,n)^5He$ reaction and followed by a decay $^5He \rightarrow n + ^4He$. For fast tritons the angular distribution of α -particles is predominantly forward and backward along the direction of motion of the 5He nucleus, thus the energy spectrum is peaked at both the maximum and minimum energies. Note that the cross-section of the $T(T,2n)^4He$ fusion reaction is continuously increasing with triton energy.

The T - T α -particle losses were studied in the high-performance T -plasma discharges. In figure 7 one can see the FILD footprint of losses recorded in the hybrid discharge #99151. There are two spots of losses on the scintillator plate, which evidence indicates are related to α -particles. The high-energy losses are spotted within gyro-radius $r_{gyr} \approx 8 - 12$ cm, the low-energy loss spot lie at $r_{gyr} < 4$ cm. The energy distribution function of the α -particle losses obtained by integrating the CCD output along $\theta = 60^\circ$ has a broad peak at ≈ 4 MeV and low-energies, $E_\alpha < 1$ MeV. These observations confirm the strong angular-distribution of T - T α -particles and can be used for studies of the $T(T,2n)^4He$ reaction physics that is important issue for astrophysics.

6. FUSION GAMMA-RAY MEASUREMENTS

Beside the $D(T,n)^4He$ reaction, which is releasing energy $Q=17.59$ MeV distributed between neutron (14.1 MeV) and α -particle (3.5 MeV), there is a radiation capture reaction, $D(T,\gamma)^5He$, with $Q=16.85$ MeV, which is also an indicator of fusion energy and α -particle production. Thus, spectrometry of 17-MeV gammas can be complementary to 14-MeV neutron measurements. Radiation capture reactions are unique for the fusion rate monitoring in the case aneutronic fusion i.e., D - H , T - H and 3He - D , or advanced fuel scenarios such as Li - H and B - H [8]. Also, some these reactions can be used for measurements both temperature and fuel ratio in the plasma core [28]. During the T -plasma studies, 20-MeV γ -rays from $T(H,\gamma)^4He$ reaction ($Q=19.8$ MeV) were measured for first time in tokamak experiments. Due to an energetic population of H -ions generated during ICRF minority

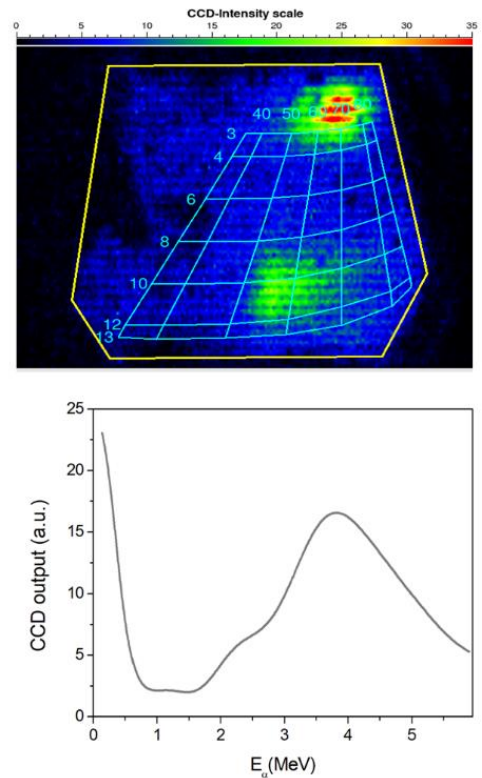


Figure 7. FILD CCD camera image recorded in TT -discharge #99151 (top box); energy distribution function of α -particle losses obtained by integrating the CCD output along pitch-angle $\theta = 60^\circ$ (bottom box).

heating of the T -plasma, the Doppler broadening of the 20-MeV γ -ray line has been observed. The spectra recorded with vertical and tangential γ -ray spectrometers is presented in figure in figure 8.

Potentially, this reaction can be used for the core temperature measurement in reactor plasmas [28, 29]. Indeed, the γ -ray spectrum of the radiative capture reaction $T(p,\gamma)^4\text{He}$ is quite sensitive to the distribution function of D - D fusion protons. An effective electron temperature could be deconvoluted from the line broadening. It can be done with rather high accuracy since a negligible background in this γ -ray energy range.

The radiation capture reaction, $D(T,\gamma)^5\text{He}$, is a weak branch of the main the $D(T,n)^4\text{He}$ fusion reaction (the branching ratio $\sim 10^{-5}$), however detection of these fusion γ -rays is important as it provides direct information on the fusion/ α -particles rate and could be utilised for this purpose in

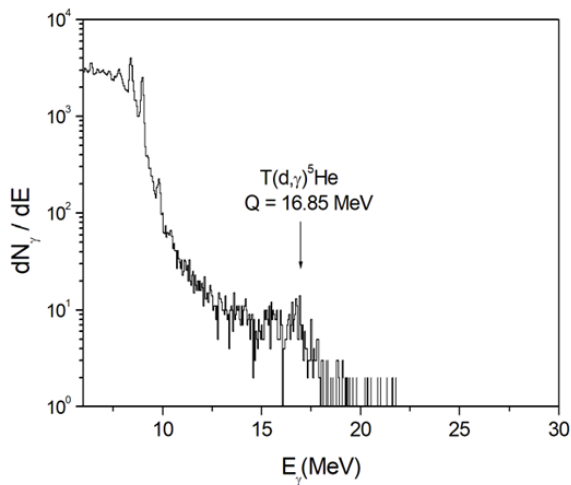


Figure 9. Gamma-ray spectrum recorded by tangential γ -ray spectrometer in the JET D -(T) plasma discharge.

sight γ -ray attenuation factors. Furthermore, both the ground state and the first excited state of the final ^5He -nucleus are rather broad i.e., the ground state width $\Gamma_{g.s.} \sim 0.6$ MeV; the first excited state width was obtained from a complicated R-matrix model calculation. Also, the 17-MeV γ -ray detector response function need to be characterised. It is known that response function of any solid-state γ -ray detector consists of a continuous γ -ray Compton scattering spectrum and three peaks: the full energy, E_γ , the single escape, $E_\gamma - m_e c^2$ and the double escape, $E_\gamma - 2m_e c^2$. Hence, deconvolution of the detected complex 17-MeV γ -ray emission is challenging and may be rather uncertain. It becomes obvious from the γ -ray spectrum, which is presented in figure 9.

Nevertheless, the 17-MeV γ -ray rate can be useful if this rate in a selected energy window is calibrated with the D - T -neutron rate provided by JET fission chambers. Then, this information can be used as an additional (or spare) tool for monitoring of the D - T fusion rate/power during discharges. Figure 10 shows yields of the γ -rays in the energy window 15 – 17.5 MeV, which are normalised to the D - T neutrons, in several discharges with low tritium concentration that prevents possible uncertainties at very high count-rates. A statistical error of the fitting is below 10% though the $D(T,\gamma)^5\text{He}$ reaction rate in these discharges was rather low. The statistical uncertainties can be reduced with an optimal diagnostic setting. So, the example presented in figure 10 demonstrates feasibility of the

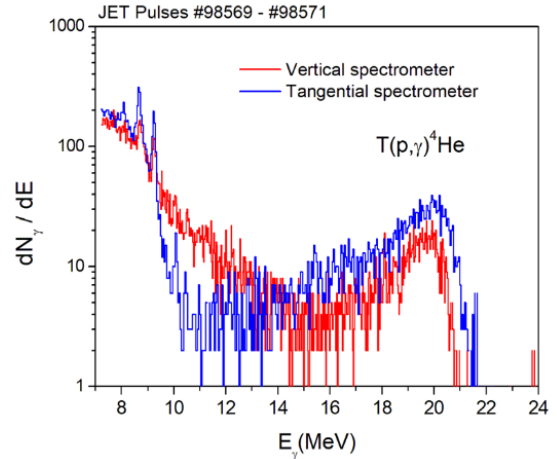


Figure 8. Integrated γ -ray spectra recorded by LaBr_3 -detectors in the T -plasmas during the H -minority heating.

reactors. Unfortunately, the absolute value of the $D(T,\gamma)^5\text{He}$ reaction-rate cannot be measured with accuracy as good as the 14-MeV neutron-rate measurements; the JET fission chambers with the calibration uncertainty $\sim 4\%$ [30] are demonstrating an accurate data on the D - T fusion rate/power.

Indeed, there are several obstacles to do the same with 17-MeV gammas from $D(T,\gamma)^5\text{He}$ reaction. The main problem is uncertainty of the reaction branching ratio, which is known with accuracy 30-50%; second one is difficulty of a precise quantification of the γ -ray diagnostic response function. Actually, several factors should be quantified for that with a required accuracy, including the plasma field-of-view and the line-of-

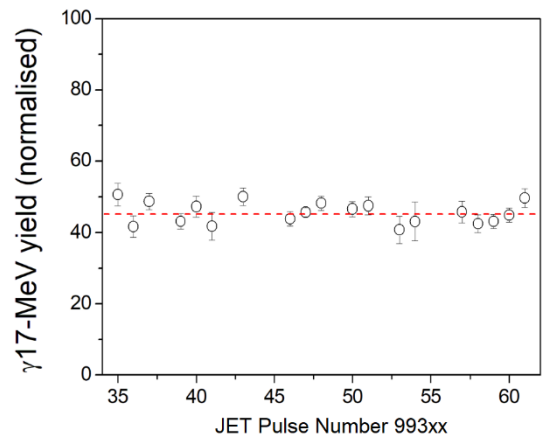


Figure 10. Vertical spectrometer yield of 17-MeV γ -rays (a.u.) normalized to the calibrated D - T neutron yield in JET pulses; dash line shows the fitted average ratio.

additional tool for the D - T fusion rate monitoring, which could be used i.e., in an emergency case if the fission chambers are failed.

7. SUMMARY AND CONCLUSIONS

Confinement of the fast α -particles produced in fusion reactions is of crucial importance for reactors. Plasma MHD instabilities may lead to significant α -particle losses and the loss of plasma heating. Selected new results of α -particle observation in DTE2 presented in this paper.

The α -particle self-heating effects were observed in the high-performance discharges with NBI power afterglow. In the D - T discharge the core electron temperature is about 30% higher than in the reference deuterium discharge. After the NBI power turned off, α -particles continue transfer their kinetic energy to plasma electrons during slowing down. The presented direct evidence of α -particle heating, which confirms conclusions of former D - T experiments, is crucial for developments of burning plasma reactors. Also, the α -particle loss effects related to MHD activities in T - and D - T plasmas were presented. Some important measurements were carried for the first time in tokamaks. Indeed, the fusion 17-MeV γ -rays due to the $D(T,\gamma)^4He$ reaction as well as 20-MeV γ -rays of the $T(H,\gamma)^4He$ reaction, were measured in D - T and tritium plasmas with the H -minority heating.

JET DTE2 experiments provided unique information on the α -particle behaviour in the ITER relevant scenarios. It gives opportunity for the detailed analysis and modelling that could enrich the knowledge on the α -particle physics in fusion reactors with magnetic confinement.

ACKNOWLEDGEMENTS

This work has been carried out within the framework of the EUROfusion Consortium, funded by the European Union via the Euratom Research and Training Programme (Grant Agreement No 101052200 — EUROfusion) and from the RCUK Energy Programme (grant number EP/W006839/1). Also, this work partially supported by the U.S. Department of Energy under contract number DE-AC02-09CH11466. Views and opinions expressed are however those of the author(s) only and do not necessarily reflect those of the European Union or the European Commission. Neither the European Union nor the European Commission can be held responsible for them. To obtain further information on the data and models underlying this paper please contact PublicationsManager@ukaea.uk.

REFERENCES

- [1] Strachan J. D. et al, 1997 Plasma Phys. Control. Fusion **39** B103
- [2] Keilhacker M. et al, 1999 Nucl. Fusion **39** 209
- [3] Kiptily V.G. et al, 2023 Phys. Rev. Lett. **131** 075101
- [4] Zastrow K.-D. et al, 2004 Plasma Phys. Control. Fusion **46** B255
- [5] Kiptily V.G. et al, 2022 Plasma Phys. Control. Fusion **64** 064001
- [6] Adams J.M. et al, 1993 Nucl. Instr. Meth. Phys. Res. **A329** 277.
- [7] Jarvis O.N. 1997 Plasma Phys. Control. Fusion **39** 1571
- [8] Kiptily V.G., Cecil F.E. and Medley S.S., Plasma Phys. Control. Fusion **48** (2006) R59
- [9] Curuia M. et al, 2017 Fusion Eng. and Design **123** 749
- [10] Nocente M. et al, 2010 Rev. Sci. Instrum. **81** 10D321
- [11] Darrow D. S. et al, 2004 Rev. Sci. Instrum. **75** 3566.
- [12] Bonfiglio P.J. et al, 2020 Rev. Sci. Instrum. **91** 093502
- [13] Baumel S. et al, 2004 Rev. Sci. Instrum. **75** 3563.
- [14] Rivero-Rodriguez J.F. et al, 2021 Rev. Sci. Instrum. **92** 043553
- [15] Kiptily V.G. et al, 2018 Nucl. Fusion **58** 014003
- [16] Hawryluk R.J. et al, Phys. Rev. Lett. **72** (1994) 3533
- [17] Taylor G. et al, 1996 Phys. Rev. Lett. **76** 2722
- [18] Thomas P.R. et al, Phys. Rev. Lett. **80** (1998) 5548
- [19] Stix T.H., Plasma Phys. **14** (1972) 367
- [20] Breslau J. et al, TRANSP, USDOE Office of Science, Fusion Energy Sciences, DOI: 10.11578/dc.20180627.4, 2018
- [21] Hobirk J. et al, Nucl. Fusion Special Issue on JET T & D-T, 2023
- [22] Garzotti L. et al, Nucl. Fusion Special Issue on JET T & D-T, 2023
- [23] Sharapov S.E. et al, Nucl. Fusion Special Issue on JET T & D-T, 2023
- [24] Kazakov Ye. et al Physics of Plasmas **22** (2015) 082511
- [25] Kiptily V.G. et al. Nucl. Fusion **49** (2009) 065030.
- [26] Yu. Baranov et al, EuroPhysics Conf. Abstracts Vol. **34A** P5.141, 37th EPS Conf. on Plasma Physics, Dublin, 2010.
- [27] Bonfiglio P.J. et al, this conference, IAEA-EX-W/1991
- [28] Kiptily V.G. et al, 2015 Nucl. Fusion **55** 023008.
- [29] Kiptily V.G. et al 2010 Nucl. Fusion **50** 084001
- [30] Batistoni P. et al 2018 Nucl. Fusion **58** 106016